Available online at www.sciencedirect.com

SCIENCE DIRECT

Cement and Concrete Research 35 (2005) 2252–2260

Cement and Concrete Research

Investigation of the microstructure and carbonation of $C\bar{S}A$-based concretes removed from service

Liang Zhang, Fredrik P. Glasser*,[1]

Department of Chemistry, University of Aberdeen, Meston Walk, Aberdeen, AB24 3UE, Scotland, United Kingdom

Received 23 December 2003; accepted 2 August 2004

Abstract

The microstructure, mineralogy and depth of carbonation of two concrete samples, one removed from a normal strength crane column and the other from a high-strength pile, are reported. The normal strength $C\bar{S}A$ cement concrete had a high w/c ratio; microstructural images show that clinker tends to hydrate almost completely. But for high-strength $C\bar{S}A$ cement concretes, made with low w/c ratios, large amounts of partially hydrated clinker grains remain as a microaggregate.

$C\bar{S}A$ cements and concretes are subject to carbonation in service conditions. The usual method of determining depth of carbonation, the phenolphthalein test, does not work with aged $C\bar{S}A$ matrices. A new method, using infrared microscopy, has been used to determine carbonation depth of aging $C\bar{S}A$ cement concrete. It has been shown that carbonation of a normal strength $C\bar{S}A$ cement concrete exposed to open air for 16 years averages ~0.5 mm/year, and is thus comparable with reported rates of carbonation of OPC concretes. The high-strength $C\bar{S}A$ concrete carbonated at a maximum rate of ~60 μm/year.

Keywords: Calcium sulfoaluminate cement; Carbonation; Infrared microscopy

1. Introduction

In the 1970s, research on the coexistence of calcium sulfoaluminate ($C_4A_3\bar{S}$) with other minerals resulted in the discovery of the practical value of those novel cement formulations [1]. A new type of cement based on $C_4A_3\bar{S}$, C_2S and ferrite, shorthand calcium sulfoaluminate, or $C\bar{S}A$ cement, has been developed in China. Other types of clinker containing $C_4A_3\bar{S}$ are known, but we report on the Chinese product containing ca. 20–25% each of $C_4A_3\bar{S}$, belite, and ferrite. This clinker is normally interground with 10–15% gypsum.

In comparison with Portland cements, production of $C\bar{S}A$ cements is small, ca. 1 million tonnes per year. But due to their balance of unique properties they are an alternative to Portland cements in some applications where the performance of Portland cement is insufficient. The unique properties of $C\bar{S}A$ cements include rapid strength development even at low temperatures, good resistance to freezing during hydration and in service conditions, good corrosion resistance and excellent durability in aggressive water, e.g., sea water. However, structural uses of $C\bar{S}A$ cements outside China are relatively uncommon and are largely confined to special cements used in non-structural applications.

C–S–H and ettringite are the main hydrates and strength-giving components of $C\bar{S}A$ cements. Many researchers have expressed concern about the long-term stability and supposed rapid rate of carbonation of ettringite-based matrices [2–4]. Zhang et al. [5] reported results from an accelerated experiment on short-term $C\bar{S}A$-based concrete samples made in the laboratory, in which no significant

* Corresponding author. Tel.: +44 1224 272906; fax: +44 1224 272903.

E-mail address: f.p.glasser@abdn.ac.uk (F.P. Glasser).

[1] Current address: National Starch and Chemical (Shanghai) Ltd., No. 137, Jiangtian East Road, Songjiang Industrial Estate, Shanghai, China (Post code: 201600).

0008-8846/$ - see front matter © 2004 Elsevier Ltd. All rights reserved.
doi:10.1016/j.cemconres.2004.08.007

differences in carbonation trends were found relative to equivalent Portland cement concretes. However, laboratory and field investigations often differ, and, in any event, it is difficult to establish a basis for equivalence between different cement types. No relevant literature has been found about microstructure and carbonation of C$\bar{S}$A-based concrete formulated with high $C_4A_3\bar{S}$-containing cements, and the resulting changes to the microstructure occurring under normal service conditions.

Phenolphthalein indicator is commonly used to determine the carbonation depth of Portland cement concrete. The method is also applicable to fresh high alumina cement (HAC) concretes to 2 years age, according to Dunster et al. [6]. However, they found that the visible indication is often indistinct and fades with time for more highly carbonated HAC concretes, both young and aged. Phenolphthalein is therefore not useful to determine carbonation depth in aged HAC concretes and the same was found to be true for aged C$\bar{S}$A cement concretes. Obviously, another method is required to evaluate the carbonation of C$\bar{S}$A cement concretes, particularly if it is also applicable to concretes made with limestone aggregates.

Depth of carbonation can also be determined by thermogravimetric analysis (TGA) using drill cuttings or diamond-sliced cores obtained at successively greater depths. Critical comparison of depths of carbonation determined by TGA and phenolphthalein reveals that the carbonation front in OPC is complex and often not sharp [7], and that direct comparison of carbonation depths is not straightforward. However, TGA is not portable and is unsuited for field investigations; moreover in the presence of carbonate aggregate, the paste fraction has to be handpicked under a binocular microscope prior to carbonate determination.

In this paper, research on samples removed from long-term service was made by SEM, XRD and IR micro-spectroscopy. The specimens were recovered from a normal strength crane column and a high-strength pile, believed to be typical of the range of uses of C$\bar{S}$A cements. Application of infrared microscopy to determining depths of carbonation is a novel technique and is described in detail.

2. Sampling

2.1. Normal strength concrete sample from a crane column

Shijiazhuang (SJZ) Special Cement Plant, located in north China, has been producing C$\bar{S}$A cements since 1974. Rapid-hardening C$\bar{S}$A cement from this plant was used for concrete structures beginning around the end of the 1970s. The column described here was concreted during the cold winter of 1982 with hot mix water. The w/c ratio was relatively high, approximately ~0.55–0.60; 1% $NaNO_2$ was also added to the mix water as an anti-freeze. The rapid-hardening C$\bar{S}$A cement content, formulated without limestone filler, was about 300–350 kg/m^3 and the 7-day compressive strength of the concrete was about 30 MPa. The column has been fully exposed to weathering in outdoor temperatures in the range ~−15 to +45 °C, enduring freeze–thaw, rain, etc. The concrete crane structure was in regular service when cored and showed no visual signs of deterioration.

The cross section of the column is about 40×40 cm. A cylindrical sample core was drilled from the crane column in September 1997. The specimen was then covered with adhesive duct tape, except for the top surface which had been exposed to air in course of service, and was thereafter stored at normal ambient temperature until examined in 2001.

2.2. High-strength concrete sample from a pile

This pile was trial-produced in June 1993 in Guangzhou (GZ), south China. The 3-day compressive strength of this concrete was required to reach 80 MPa. The objective of using C$\bar{S}$A cement to produce this kind of pile was to eliminate the need for lengthy or complex curing. An iron-rich C$\bar{S}$A clinker was used, produced in a special cement plant in south China and formulated without added gypsum. Medium sand with very low clay content and 5–20-mm crushed granite were used as aggregates; river water was used as mix water. In order to lower the w/c ratio and prolong setting time, superplasticiser and retarder were added to the fresh concrete mix: the cement content was 500 kg/m^3. The w/c ratio was normally controlled to ~0.30 but could be reduced to as low as ~0.26 because centrifugal casting was used. The production process of a cylindrical pile is as follows: initially fresh concrete is fed into the two halves of a clamped steel mould and prestress applied, followed by centrifugation, precuring, demoulding and secondary curing. The curing regime for C$\bar{S}$A cement piling was to precure piles for 7–8 h prior to demoulding, followed by water curing at ambient temperature for 3 days, by which time compressive strengths exceeded 80 MPa. Secondary curing was uncontrolled. The temperature inside the pile during precuring reached ~50 °C. The C$\bar{S}$A cement piles were stored outdoors for more than 1 year. Part of a pile produced in June, 1993 was cut off and transported to Beijing. It was kept outdoors unprotected from the weather until 1998, when a portion was sent to Aberdeen and examined in 2001. Visually, the pile was in perfect condition.

3. Experimental

3.1. Specimen preparation for SEM and XRD investigation

The specimens were prepared for backscattered electron (BSE) imaging by embedding the sample in epoxy resin blocks. The blocks were ground down using progressively finer grade abrasive papers and then polished to a surface roughness of <1 μm (using 6 μm diamond paste, followed by ¼ μm alumina paste as the polishing medium). The samples were coated with a thin layer of conductive carbon. Powdered

samples intended for X-ray diffraction (XRD) were collected by selectively crushing concrete specimens and removing as much aggregate as possible by hand picking. The resulting powders were dispersed on a glass slide for X-ray diffraction analysis. The powder was adhered to the slide by a thin layer of "Vaseline" because only a small quantity of paste-rich material was available.

3.2. Infrared spectroscopy and sample preparation

The infrared spectrum is generally regarded as one of the most characteristic properties of a compound. Although used routinely by organic chemists, it is perhaps less often used in inorganic chemistry. Nevertheless, this technique proved useful to characterise of carbonation depth of $C\bar{S}A$ cement samples.

The infrared region of the electromagnetic spectrum lies between the microwave and visible and extends from wavelengths of 0.75 to 200 μm, although only part of this range is normally used to obtain infrared spectra, typically 400–4000 cm^{-1} (2.5–25 μm). When a sample is irradiated by an infrared beam whose frequency is changed progressively, the constituent molecule or group, in this instance carbonate, will absorb certain frequencies corresponding to energy consumed in stretching or bending different bonds. The transmitted or reflected beam corresponding to the region of absorption will be weakened, and thus a recording of the intensity of the transmitted or reflected beam versus wave-numbers or wavelength will give a curve showing absorption bands [8]. With appropriate sources, IR transparent optics and an imaging system, optical microscopy in the IR region becomes practicable: a Nicolet Continuum microscope was used. The method has not previously been applied to cements, so it was necessary to develop the technique.

The procedure is shown in Fig. 1. A flat piece of concrete was cut in the desired orientation, using a diamond saw, from the concrete sample. This was cohered onto a 7.5×2.5-cm glass slide, using an IR transparent glue, the slide having previously been coated with gold. The gold layer serves as a total reflectance coating and increases the optical path length without

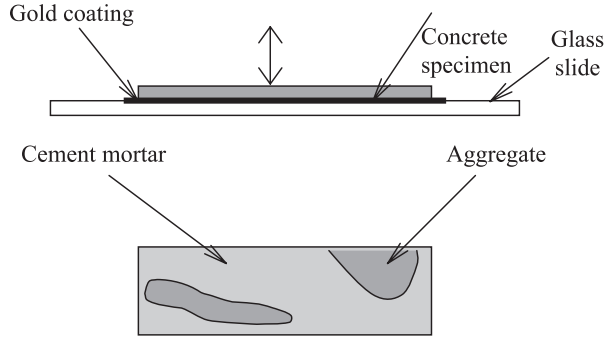

Fig. 1. A slice of concrete prepared for infrared spectroscopy. Top, cross-section and bottom plan view. The double arrow shows the direction of the incident and reflected IR beam.

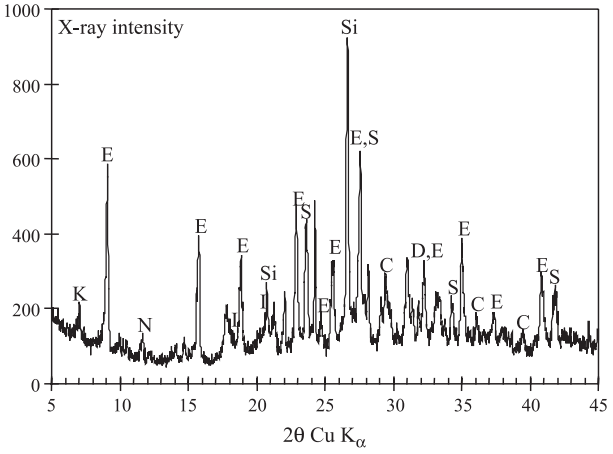

Fig. 2. XRD diagrams of the specimen from the crane column of SJZ, 16 years. N—$C_4A\bar{C}H_{11}$; S—$C_4A_3\bar{S}$; E—ettringite; I—AH_3; D—C_2S; K—C_2ASH_8; C—$CaCO_3$; Si—SiO_2.

significant loss of resolution. The sample was polished to 10–15 μm thickness without a cover slip. Prepared specimens were stored in a vacuum desiccator to avoid further carbonation. Typically, a 32× infrared transparent objective was used and each side of the reticule reference square measured 47 μm: the full field of view was ~656 μm in diameter. The practical limit of lateral resolution is limited by the optics, by signal intensity, as well as by surface roughness and lateral scatter of the beam within the specimen. In the present application, the lateral resolution was ~50 μm. Finer resolution was possible, but only with sacrifice of signal strength and consequent degradation of signal/noise ratio.

4. Results

4.1. Investigation of normal strength concrete sample from the crane column

XRD patterns of the specimen from the crane column are shown in Fig. 2. Except for SiO_2 and $CaCO_3$ which come

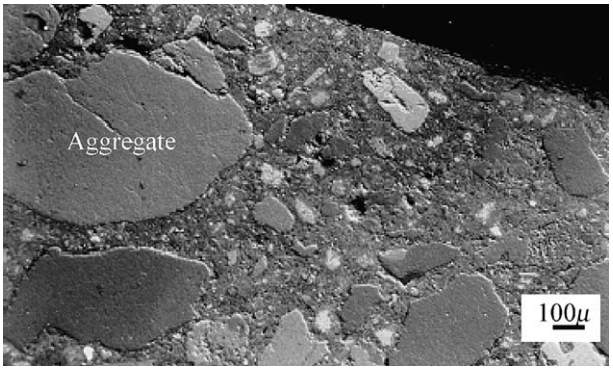

Fig. 3. General view of the microstructure of near surface concrete from the crane column of SJZ, 16 years. The air interface is at the upper right hand side (black).

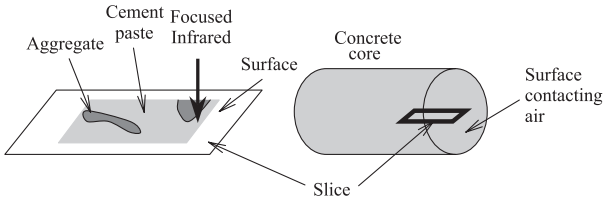

Fig. 4. Concrete slice preparation for carbonation assessment, from crane column of SJZ, 16 years old. Ink marks are used to preserve the orientation relationships.

from the aggregates, the major hydration product identified in the paste is ettringite; AH_3 (gibbsite), and C_2AS_8 together with traces of $C_4A\bar{C}H_{11}$ are also present. Wang et al. [9] attributed formation of C_4ACH_{11} to the reaction between calcium carbonate, often added as a filler or present as an impurity in gypsum, and $C\bar{S}A$ cement paste. Minor calcium sulfoaluminate and C_2S also remain. Fig. 3 shows a general view of the microstructure of near-surface concrete from the crane column. The larger grey or dark grey particles are aggregate, which are comprised of a mixture of fine silica sand and coarser limestone. The small bright spots are residual clinker grains.

Infrared spectroscopy was used to investigate the carbonation depth. Choosing the correct spot size is important to obtain the required information. If too large a spot is chosen, both aggregate and cement paste will be included and, because the coarse aggregate was $CaCO_3$, false information will result when assessing carbonation of the paste component. On the other hand, if the spot is too small, the reflecting signal will be too weak for accurate determinations. The spot size used in this work, as optimized empirically, was about 50 μm diameter. According to the BSE images shown in Fig. 3, regions of cement paste between calcium carbonate coarse aggregate are sufficiently large to accommodate this beam spot size without overlapping onto aggregate particles while, at the

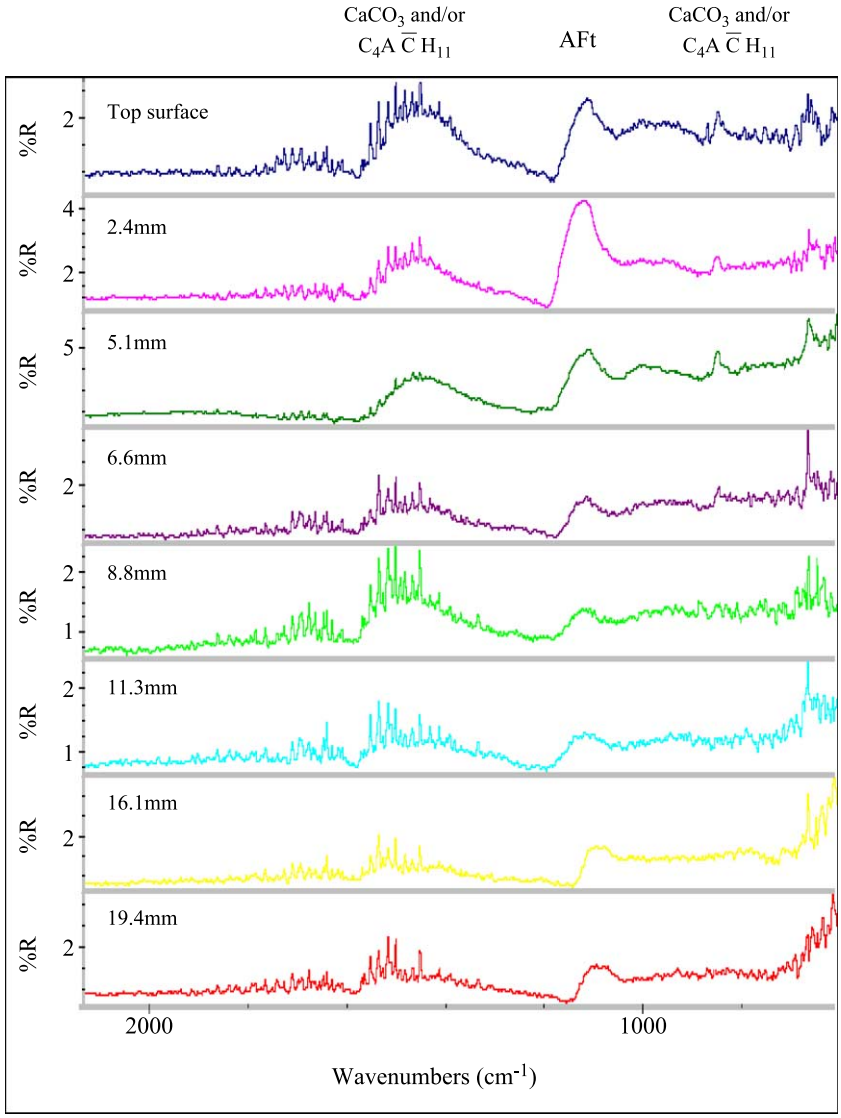

Fig. 5. IR spectra profiles of a crane column of concrete from top surface to interior paste, 16 years old. The distances marked are depths from the top surface (exterior). The signal below ~900 cm^{-1} is much influenced by noise.

same time, give a satisfactory signal intensity. With more experience, it should be possible to reduce the spot size to 20–30 μm.

In order to assess depths of carbonation, specimen orientation was controlled, as shown in Fig. 4. A line from the top surface to interior paste was carefully located so as to provide an aggregate-free path thus enabling the beam to traverse only cement paste. IR spectra from several points on a level horizontal line parallel to the surface were sometimes included and were compared with each other so as to verify the local background intensity, free from interferences. The optical images and beam positioning were individually focused by hand, and spectra from selected points were frequently repeated several times to confirm reproducibility. A typical scan is shown in Fig. 5. Major phases were determined by XRD (Fig. 2) and, with the aid of reference IR spectra reported by Farmer [10], ettringite, SiO_2, (quartz) $CaCO_3$ (calcite) and $C_4A\bar{C}H_{11}$ could be identified by their IR spectra; characteristic major vibrational frequencies in the region 500–2000 cm^{-1} as reported in the literature [10,11] are given in Table 1. The spectral component attributed to ettringite at 1120 cm^{-1} occurs throughout. The reflectances at ~870 , ~1440 and ~1600 cm^{-1} correspond either to $CaCO_3$ or $C_4A\bar{C}H_{11}$, or both. The two minerals are very likely produced by partial carbonation of $C\bar{S}A$ cement paste as well as by reaction with $CaCO_3$ fines derived from aggregate. In this context, it is noteworthy that even granite aggregates may contain $CaCO_3$ as an accessory mineral and, in concrete from the crane column, calcite was probably present in gypsum [8]. Therefore, reflectance maxima typical of carbonates may appear even in cement paste from the interior but their presence does not necessarily indicate atmospheric carbonation. At first sight, these considerations might appear to limit application of the IR method to determine depths of carbonation, but even in the presence of carbonate we can still measure how reflectance maxima of $CaCO_3$ and/or $C_4A\bar{C}H_{11}$ change with depth from the top surface to the interior from absorption intensities in the IR spectra. Fig. 5 records large decreases in carbonate absorptions that mark the carbonation front; distances marked in the figures are depths from the original exposed surface with air.

Table 1
Some vibrational frequencies in the region 500–2000 cm^{-1} of possible minerals in concrete [9,10]

Minerals	Vibrational frequencies (cm^{-1})
$CaCO_3$	872, 1420, 710
SiO_2	798, 1084, 697
$C_4A\bar{C}H_{11}$	878, 1474, 1660
Ettringite	~1120
$C_4A_3\bar{S}$	~650, ~750, ~1100, ~1200

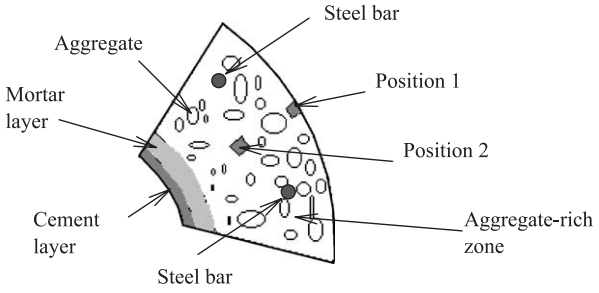

Fig. 6. Sampling positions from a high-strength pile at GZ, 5 years. The pile is hollow and the layering results from centrifugation.

Percent reflectance shows the amount of infrared energy reflected from the sample and is defined by the equation

$$\%R = (IS/IB) \times 100$$

where IS is the intensity of infrared energy reflected from the sample and IB is the intensity of infrared energy passing through the reflection accessory without a sample in place. Using the method of selective positioning of the beam, as described above, the maxima of $CaCO_3$ and/or $C_4A\bar{C}H_{11}$ in the crane column abruptly become quite weak in the depth range greater than 8.8–10 mm, but less than 11.3, implying carbonation rates on the order of 0.4 to 0.5 mm/year. Supplementary X-ray examination of selected regions discloses that carbonation does not totally destroy ettringite to any significant extent except very close to the surface at depths not exceeding ~1 mm. Reasons for this are discussed subsequently.

4.2. Investigation of a high-strength concrete sample from the pile

Two pieces of sample were broken from two different positions of the pile, as shown in Fig. 6. The powder samples used for XRD investigation were taken from

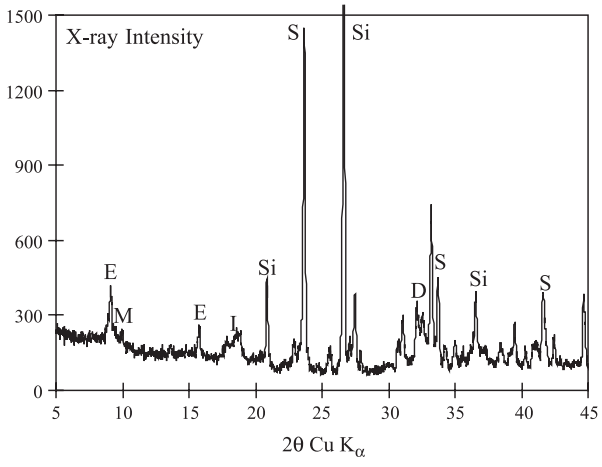

Fig. 7. XRD diagrams of the specimen from a high-strength pile after 5 years. E—ettringite; M—monosulfate; I—AH_3; S—sulfoaluminate; D—C_2S; Si—SiO_2 (quartz), arising from sand.

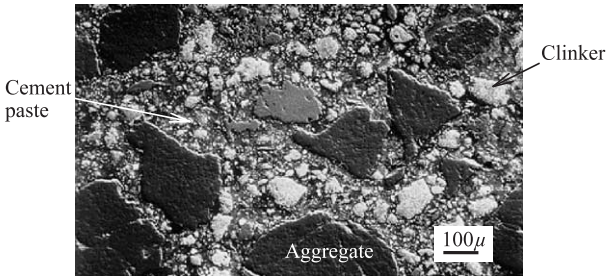

Fig. 8. General view of the microstructure from a high-strength pile of GZ, 5 years.

position 2. XRD analyses of the cement paste (Fig. 7) revealed ettringite, monosulfate, AH_3 and substantial amount of unhydrated sulfoaluminate clinker; both $C_4A_3\bar{S}$ and β C_2S were detected. Fig. 8 shows the microstructure of the pile, position 2, at low magnification. Large, dark grey particles are aggregates while optically bright grains are partially hydrated clinker. The microstructure is very dense; the few voids which can be observed are air bubbles and honeycomb-like regions. The microstructure at position 1 is shown in Fig. 9. A leached layer has developed at the outermost surface extending to depths of 0.1–0.2 mm. From the magnified image (Fig. 10), clinker grains in this near-surface layer, marked with a dotted line, have almost completely hydrated with only ferrite and perovskite phases remaining.

A slice cut from the specimen in position 1 was used to investigate depth of carbonation. From the BSE image (Fig. 9), although less cement paste is present than in the crane column specimen due to aggregate segregation during centrifugation, a spot size of 50 μm is still satisfactory to obtain a line scan spectrum from the paste by careful positioning. The IR spectra of different points from top surface to interior paste are shown in Fig. 11. Obviously, from the intensity of carbonate sorptions, the outer surface of the pile has been carbonated. By combining X-ray and IR spectra data obtained from the top surface, the sorptions of AFt can be seen to disappear while $CaCO_3$ appears. At depths between 40 and 254 μm from the top surface, the maxima of the response due to $CaCO_3$ reduce until at mean depths >351 μm, IR spectra of paste did not reveal $CaCO_3$; the major IR absorptions come from AFt and unhydrated $C_4A_3\bar{S}$, as marked in Fig. 11. Obviously, the carbonation

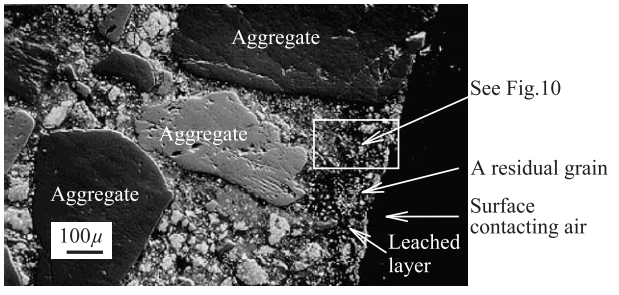

Fig. 9. General view of the near surface microstructure from a high-strength pile at GZ, 5 years.

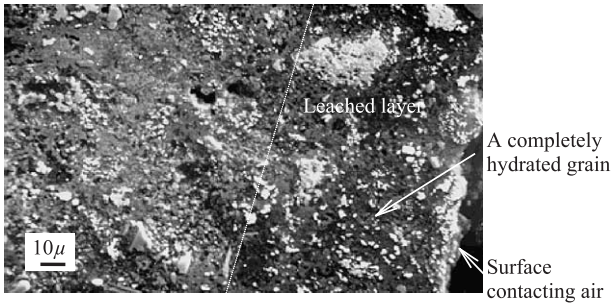

Fig. 10. Near surface microstructure from a high-strength pile, 5 years.

depth of the high-strength pile is very small, not exceeding ~300 μm. This carbonation depth implies a maximum rate of ~60 μm/year, assuming that all carbonation occurred in the course of outdoor exposure.

5. Discussion

5.1. Infrared microscopy and its relation to other methods

Although the conditions for infrared microscopy were not fully optimized, the method shows great promise in determining the geometry of the carbonation front. Not surprisingly, the method worked best in concretes that were made with non-calcareous aggregates and without limestone fillers. But somewhat to our surprise, it proved possible to obtain relevant data from concretes containing both limestone aggregate and cement which had been interground with impure, carbonate-containing gypsum.

The IR microscopy is of course not portable but it is practicable to remove field samples for laboratory analysis and specimen preparation is not much different than would be required for conventional optical microscopy. The microscope is intrinsically superior to the phenolpthaelein test in determining carbonate gradients. It should be recalled that the phenolphthalein test is pH dependent such that a colour change does not occur for Portland cement until all or virtually all $Ca(OH)_2$ and C–S–H have been carbonated. Although portlandite is absent from the $C\bar{S}A$ cements we used, pH is maintained by C–S–H, typically having Ca/Si ~1.5. A partially carbonated zone, in which some lime-rich C–S–H is preserved also occurs. Carbonation thus typically extends to rather greater depths than are revealed by the phenolphthalein test. This has been shown for Portland cement by direct comparison of chemical and thermogravimetric analysis [7]. While differences between techniques may seem academic, this is not so, particularly when data are subsequently used to construct models to predict the future rate of propagation of carbonation “fronts” into concrete with a view to making lifetime predictions for passivation of embedded steel.

The carbonation rates averaged over years of exposure assume a linear dependence on carbonation with time. With

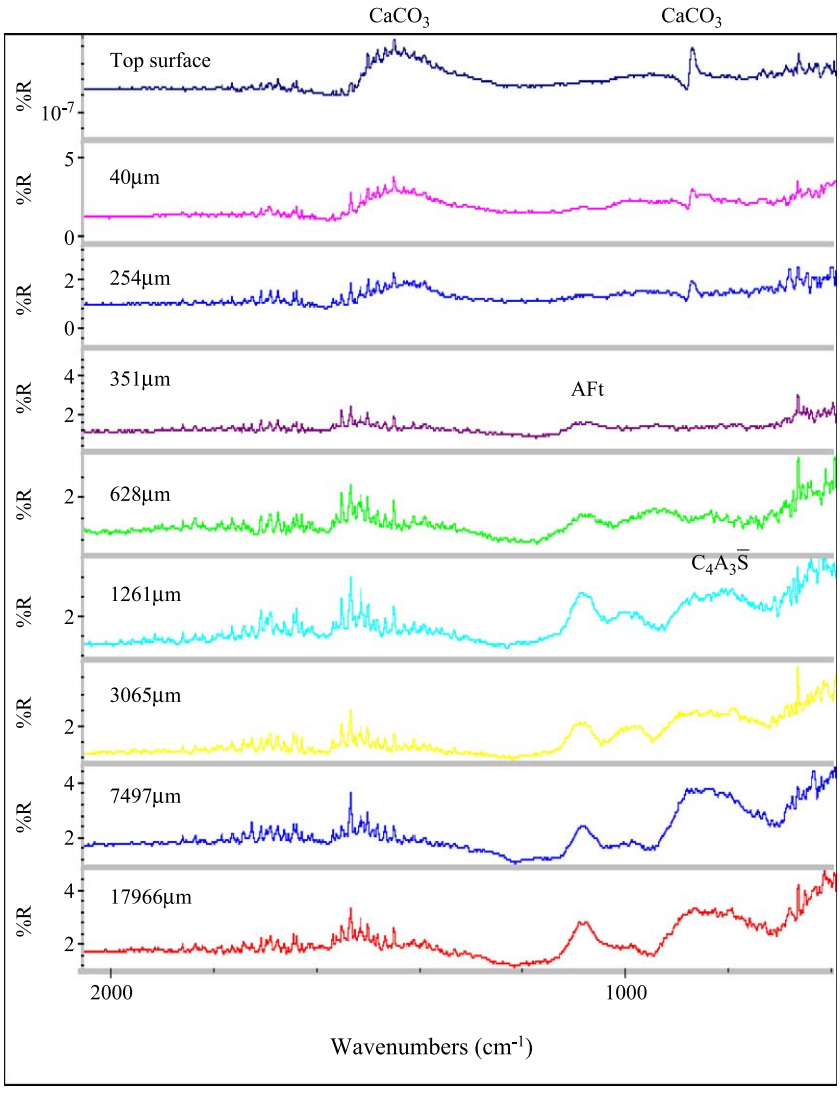

Fig. 11. IR spectra profiles of a high-strength pile at GZ from top surface to interior paste, 5 years old. The distances marked are the depth from the selected point to the top surface. Main absorptions are assigned on representative spectra.

only one measurement point in time, such a fit is reasonable but the numerical value thus obtained should not necessarily be extrapolated into the future: straightforward diffusion theory suggests that progression of carbonation to greater depth is proportional to $t^{1/2}$. Further work is required to prove this dependence.

5.2. Role of microstructure

The C$\bar{S}$A cements used in the in-service structures were mainly produced by blending gypsum with C$\bar{S}$A clinker. The hydration process and changes in microstructure have been described in Ref. [12]. The microstructure in the partially carbonated zone does not differ significantly from that of uncarbonated matrix, probably because so much ettringite is preserved. In mature C$\bar{S}$A cement paste, hydration products from the reaction of clinker and gypsum with water include ettringite, AH_3, C–S–H and C_2ASH_8. These comprise a dense matrix which envelops large, partially hydrated residual grains into a rigid paste. The porosity of the matrix at the micron to 100-nm scale depends to a great extent on the original w/c ratio, other factors being approximately equal.

The water content specified to formulate concrete depends on workability and slump specifications. Lower water contents are readily achieved by using plasticisers for both C$\bar{S}$A and OPC types. However, the bulk of OPC concrete is still unplasticised, or lightly plasticised, with the result that most Portland cement concretes are made to w/c ratios >0.40. As a consequence, we normally expect to encounter water-filled pores. However, C$\bar{S}$A cements require a higher w/c ratio than Portland cement to achieve complete hydration; probably 0.45–0.50 for the cement types used in the crane column and pile. It is therefore commonplace to find unreacted clinker in C$\bar{S}$A cements due to the much higher chemical water demand of C$\bar{S}$A clinkers. As a consequence of limiting the water content, the hardened concrete rapidly undergoes self-desiccation;

pores tend to be empty and, once empty, are very difficult to resaturate. Numerous experiments in our laboratories confirm this observation. Thus, it is likely that carbonation rates will not be linear functions of w/c ratios: some critical w/c threshold will occur below which carbonation rates in uncracked matrices will remain very low.

From laboratory studies, supported by investigation on the two in-service concretes described in this paper, two types of microstructure exist in hardened $C\bar{S}A$ cement pastes: (i) a porous microstructure appropriate to high w/c ratio, high porosity concretes, in which clinker tends mainly to have hydrated, (ii) a microstructure characteristic of low w/c ratio, low porosity concretes which are characterised by absence of free water in pores and the persistence of much unhydrated clinker. The first microstructure is exhibited by the low-strength crane concrete, made without admixtures, and formulated to a high w/c ratio to achieve workability. The second microstructure is relevant to high-strength concretes, typically made with superplasticiser and retarder, and in this instance cast by centrifugal technology such that the w/c ratio is reduced to very low levels at an early stage of hydration. Nevertheless, even though clinker hydration is incomplete, the hydrates formed appear to fill space very efficiently. The lower w/c ratios of cement pastes reduces and refines their porosity thus making it difficult for water and carbon dioxide to penetrate in the course of subsequent service. When the w/c ratio is reduced to such extent that little free water remains and very low porosity is reached in the paste, the residual clinker phases are almost impossible to hydrate even after prolonged (1–2 years) water immersion; the resulting microstructure and mineralogy are effectively 'frozen'.

Obviously, the two microstructures have implications for the long-term performances of $C\bar{S}A$ cement concrete. For example, carbonation rates, which relate to penetration and the availability for transport of pore solution, differ between the two regimes. The resistance to penetration depends primarily on the permeability of the concrete. High-strength $C\bar{S}A$ cement concrete has both low permeability and low porosity. These factors, coupled with the self-desiccated internal state, ensure that carbonation is mainly confined to the near surface layer. But for low strength concrete formulated to high w/c ratio, (the specimen from the crane column), carbonation extends much deeper due to the increased permeability and the presence of pore solution, both of which enhance diffusion rates.

5.3. Chemical buffer systems in $C\bar{S}A$ cements

The cement matrix has substantial chemical buffering power to resist and impede the inward diffusion of CO_2 by chemical binding. Firstly, as the activity of carbonate increases in fresh, unaltered paste, sulfate AFm is converted to monocarboaluminate. Secondly, ettringite itself undergoes anion exchange in which part of its sulfate is replaced by carbonate. This process is known to occur in the laboratory; "carbonate ettringite" is a stable phase at elevated pH and at normal service temperatures, ~20 °C. Indirect evidence suggests that the activity of CO_2 has to be quite high before ettringite finally decomposes to, amongst other phases, $CaCO_3$. A reasonable interpretation of the combined diffraction patterns and micro infrared patterns is that ettringite undergoes significant ion exchange, of CO_3 for SO_4, prior to its decomposition and thus also buffers the paste against carbonate penetration. Only after CO_2 activities reach a sufficiently high and, as yet undefined value, will ettringite irreversibly decompose.

The interpretations given above are, in part, speculative. But the slow rates of carbonation measured following outdoor exposure are real. In well-made, low w/c ratio $C\bar{S}A$ concretes, progressive carbonation is slow and experience shows that the concrete matrix will protect steel from corrosion throughout a long service life.

6. Conclusions

IR microscopy is a useful tool to examine the carbonation depth of aged CA cement concrete. The presence of carbonate as coarse aggregate or added as filler does not invalidate the method, although it reduces the sensitivity of discrimination and requires more care in application to avoid interference from $CaCO_3$ aggregate. The carbonation depth of CA cement concrete made to high w/c ratio is comparable to an OPC concrete of equivalent quality. Ettringite persists even in very near surface layers of a crane column exposed to air for 16 years; it is suggested that this is a partially carbonate-substituted ettringite. Resistance to carbonation is improved by decreasing w/c mix ratios. In well-made concretes having low w/c ratios, the carbonation front advances slowly because the matrix has undergone self-desiccation; free water in the form of pore fluid is not available to dissolve and transport CO_2. This, coupled with the low permeability of the constituent solids and their sorption potential for CO_2, slows the rate of carbonation. $CaCO_3$ is only formed towards the final stages of carbonation.

Acknowledgement

The work reported here was supported by Fosroc Construction, UK.

References

[1] L. Zhang, M.Z. Su, Y.M. Wang, Development of the use of sulfo- and ferro-aluminate cements in China, Adv. Cem. Res 11 (1999) 15–21.
[2] T. Grounds, H.G Midgley, D.V. Nowell, Carbonation of ettringite by atmospheric carbon dioxide, Thermochimica Acta 135 (1988) 347–352.

[3] T. Nishikawa, K. Suzuki, S. Ito, K. Sato, T. Takebe, Decomposition of synthesised ettringite by carbonation, Cem. Concr. Res. 22 (1992) 6–14.
[4] X.T. Chen, X.T. Zou, X.R. Chen, Kinetic study of ettringite carbonation reaction, Cem. Concr. Res. 24 (1994) 1383–1389.
[5] L. Zhang, Y.M. Wang, M.Z. Su, Control properties of sulpho- and ferro-aluminate cement with the special admixtures, 10th I.C.C.C., Proceedings, Gothenburg, Sweden, 1996, 1997.
[6] A.M. Dunster, D.J. Bigland, K. Hollinshead, N.J. Crammond, Studies of carbonation and reinforcement corrosion in high alumina cement concrete, Proceedings, Corrosion of Reinforcement in Concrete Construction, Cambridge University Press, 1996, pp. 191–199.
[7] A.A. Rahman, F.P. Glasser, Comparative studies of the carbonation of hydrated cements. Advances in Cement Res., 2, (18) 44–54.
[8] K. Nakanishi, P.H. Solomon, Infrared Absorption Spectroscopy, 2nd ed., Holden-Day, San Francisco, CA, 1977.
[9] Y.M. Wang, M.Z. Su, L. Zhang, Sulfo-aluminate cement (in Chinese), 1999, 135. ISBN 7-5639-0819-6/t.
[10] V.C. Farmer (Ed.), The Infrared Spectra of Minerals, Mineralogical Society, London, 1974.
[11] O. Henning, W. Danowski, Infrared investigation of the double salts in the system $CaO–Al_2O_3–CaSO_4–H_2O$, Proceeding of the 8th Conference of Silicate Industry, Budapest, 1965, pp. 231–234.
[12] L. Zhang, F.P. Glasser, Hydration of calcium sulfoaluminate cement at less than 4 hours, Adv. Cem. Res. 14 (2002) 141–155.